Supporting Information

In silico designed Axl receptor blocking drug candidates against Zika virus infection

Edita Sarukhanyan[1], Sergey Shityakov[2], and Thomas Dandekar[1*]

[1]Department of Bioinformatics, Biocenter, Am Hubland, University of Würzburg, 97074 Würzburg, Germany

[2]Department of Anesthesia and Critical Care, Oberdürrbacher Str. 6

University Hospital Würzburg, 97080 Würzburg, Germany

The supporting information contains:

References

We give literature references on the multiple sequence alignments involving DEAD-like helicases, E-protein C-terminal domain, RNA-directed RNA polymerases related to the different viral strains. The alignments are attached as a separate **.clw** file.

Figures S1 – S5 – representation of compounds 1-5 inside the binding pocket of Axl receptor and indicated with dashed lines the contacts between the compounds and the key amino acid residues.

Figure S6 – S8 – graphical representation of R428, compounds 1' and 2' inside the binding pocket of Axl receptor and indicated with dashed lines the contacts between the compounds and the key amino acid residues.

We give a short explanation on the approaches used in Figure S9 and S10 as well as

Figure S9 - RMSD and RMSF regarding structural stability in molecular dynamics simulation and

Figure S10 – secondary structure analysis of Axl receptor upon warfarin and compound 2' binding.

Finally, **Table S1** gives the closest distances between the compounds and the residues involved in interactions.

References

The multiple sequence alignments for the DEAD-like helicases, E-protein C-terminal domain, RNA-directed RNA polymerases related to the different viral strains are attached as a separate .clw file. Below are given some references for the Yellow Fever virus (YFV), Dengue virus (DENV), Zika virus (ZIKV), Japanese encephalitis (JEV) and West Nile virus (WNV) used in the alignment.

Reference YFV:

J Gen Virol. 2005 Jun;86(Pt 6):1747-51.

Characterization of an infectious clone of the wild-type yellow fever virus Asibi strain that is able to infect and disseminate in mosquitoes.

McElroy KL(1), Tsetsarkin KA, Vanlandingham DL, Higgs S.
DOI: 10.1099/vir.0.80746-0
PMID: 15914853 [PubMed - indexed for MEDLINE]

Dengue virus isolates were considered as follows:

Four major strains, DENV-1, DENV-2, DENV-3 and DENV-4 were compared as sequence alignment are available from NCBI protein database. We give here four references characterizing these:

Reference DENV-1
J Virol Methods. 2010 Oct;169(1):202-6. doi: 10.1016/j.jviromet.2010.06.013. Epub 2010 Jun 30.

A method for full genome sequencing of all four serotypes of the dengue virus.

Christenbury JG(1), Aw PP, Ong SH, Schreiber MJ, Chow A, Gubler DJ, Vasudevan SG, Ooi EE, Hibberd ML.
DOI: 10.1016/j.jviromet.2010.06.013
PMID: 20600330 [PubMed - indexed for MEDLINE]

Reference DENV-2
Virology. 1997 Apr 14;230(2):300-8.

Construction of infectious cDNA clones for dengue 2 virus: strain 16681 and its attenuated vaccine derivative, strain PDK-53.

Kinney RM(1), Butrapet S, Chang GJ, Tsuchiya KR, Roehrig JT, Bhamarapravati N, Gubler DJ.
DOI: 10.1006/viro.1997.8500
PMID: 9143286 [PubMed - indexed for MEDLINE]

Reference DENV-3
J Virol. 2009 May;83(9):4163-73. doi: 10.1128/JVI.02445-08. Epub 2009 Feb 11.

Genomic epidemiology of a dengue virus epidemic in urban Singapore.

Schreiber MJ(1), Holmes EC, Ong SH, Soh HS, Liu W, Tanner L, Aw PP, Tan HC, Ng LC, Leo YS, Low JG, Ong A, Ooi EE, Vasudevan SG, Hibberd ML.
DOI: 10.1128/JVI.02445-08
PMCID: PMC2668455
PMID: 19211734 [PubMed - indexed for MEDLINE]

Reference DENV-4
1. J Virol Methods. 2010 Oct;169(1):202-6. doi: 10.1016/j.jviromet.2010.06.013. Epub 2010 Jun 30.

A method for full genome sequencing of all four serotypes of the dengue virus.

Christenbury JG(1), Aw PP, Ong SH, Schreiber MJ, Chow A, Gubler DJ, Vasudevan SG, Ooi EE, Hibberd ML.
DOI: 10.1016/j.jviromet.2010.06.013
PMID: 20600330 [PubMed - indexed for MEDLINE]

Reference ZIKV
Genome Announc. 2014 Jun 5;2(3). pii: e00500-14. doi: 10.1128/genomeA.00500-14.

Complete coding sequence of zika virus from a French polynesia outbreak in 2013.

Baronti C(1), Piorkowski G, Charrel RN, Boubis L(2), Leparc-Goffart I(2), de Lamballerie X.

DOI: 10.1128/genomeA.00500-14
PMCID: PMC4047448
PMID: 24903869 [PubMed]

Reference ZIKV
Genome Announc. 2016 Mar 3;4(2). pii: e00032-16. doi: 10.1128/genomeA.00032-16.

First Complete Genome Sequence of Zika Virus (Flaviviridae, Flavivirus) from an Autochthonous Transmission in Brazil.

Cunha MS(1), Esposito DL(2), Rocco IM(1), Maeda AY(1), Vasami FG(1), Nogueira JS(1), de Souza RP(1), Suzuki A(1), Addas-Carvalho M(3), Barjas-Castro Mde L(3), Resende MR(4), Stucchi RS(5), Boin Ide F(5), Katz G(6), Angerami RN(3), da Fonseca BA(7).

DOI: 10.1128/genomeA.00032-16
PMCID: PMC4777745
PMID: 26941134 [PubMed]

Reference ZIKV
Clin Microbiol Rev. 2005 Oct;18(4):608-37.

Biological transmission of arboviruses: reexamination of and new insights into components, mechanisms, and unique traits as well as their evolutionary trends.

Kuno G(1), Chang GJ.
DOI: 10.1128/CMR.18.4.608-637.2005
PMCID: PMC1265912
PMID: 16223950 [PubMed - indexed for MEDLINE]

2. Arch Virol. 2007;152(4):687-96. Epub 2007 Jan 3.

Full-length sequencing and genomic characterization of Bagaza, Kedougou, and Zika viruses.

Kuno G(1), Chang GJ.

DOI: 10.1007/s00705-006-0903-z
PMID: 17195954 [PubMed - indexed for MEDLINE]

Reference JEV
Virus Genes. 1991 Apr;5(2):95-109

Identification of mutations occurred on the genome of Japanese encephalitis virus during the attenuation process

Aihara,S., Rao,C., Yu,Y.X., Lee,T., Watanabe,K., Komiya,T., Sumiyoshi,H., Hashimoto,H. and Nomoto,A.

Reference WNV
Virology. 2006 Jun 5;349(2):371-81. Epub 2006 Mar 20.

Biological properties of chimeric West Nile viruses.

Borisevich V(1), Seregin A, Nistler R, Mutabazi D, Yamshchikov V.
DOI: 10.1016/j.virol.2006.02.013
PMID: 16545851 [PubMed - indexed for MEDLINE

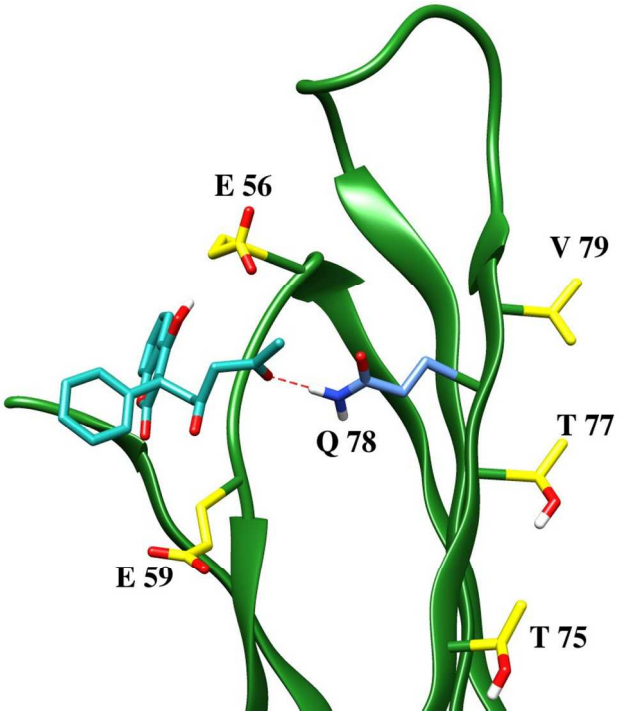

Figure S1. Compound 1 (light sea green) inside the binding pocket of Axl receptor. The receptor is shown in green as a cartoon representation. The key residues are highlighted in yellow. The residues that are different from the key residues, but are involved in contacts with the compound are shown in cornflower blue. The contacts are indicated in red dashed lines.

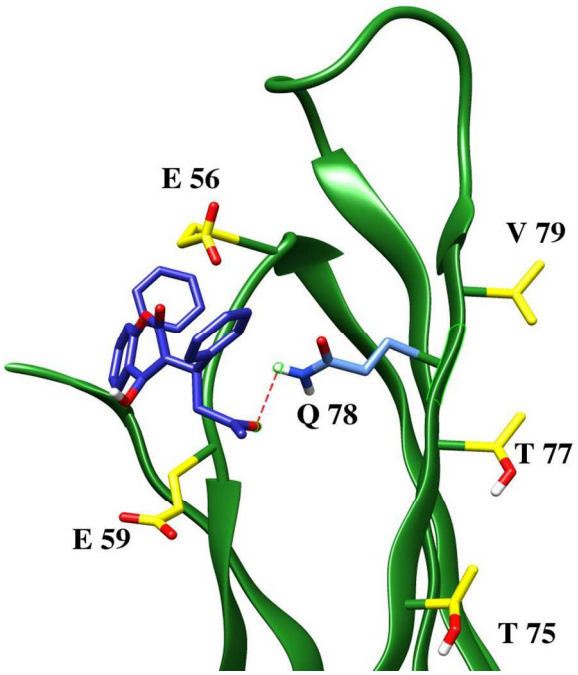

Figure S2. Compound 2 (medium blue) inside the binding pocket of Axl receptor. The receptor is shown in green as a cartoon representation. The key residues are highlighted in yellow. The residues that are different from the key residues, but are involved in contacts with the compound are shown in cornflower blue. The contacts are indicated in red dashed lines.

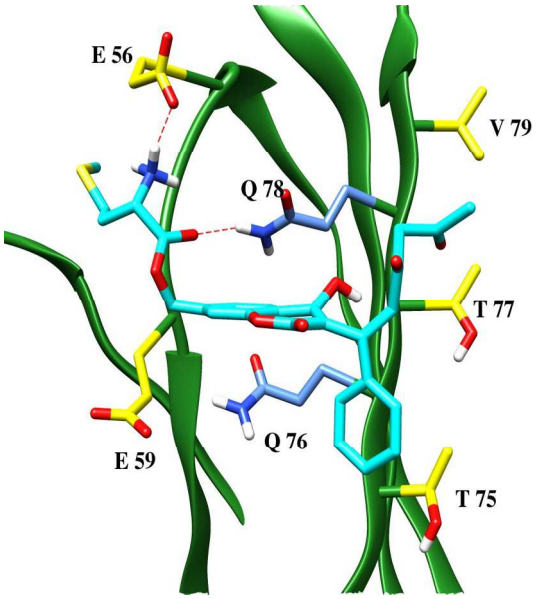

Figure S3. Compound 3 (cyan) inside the binding pocket of Axl receptor. The receptor is shown in green as a cartoon representation. The key residues are highlighted in yellow. The residues that are different from the key residues, but are involved in contacts with the compound are shown in cornflower blue. The contacts are indicated in red dashed lines.

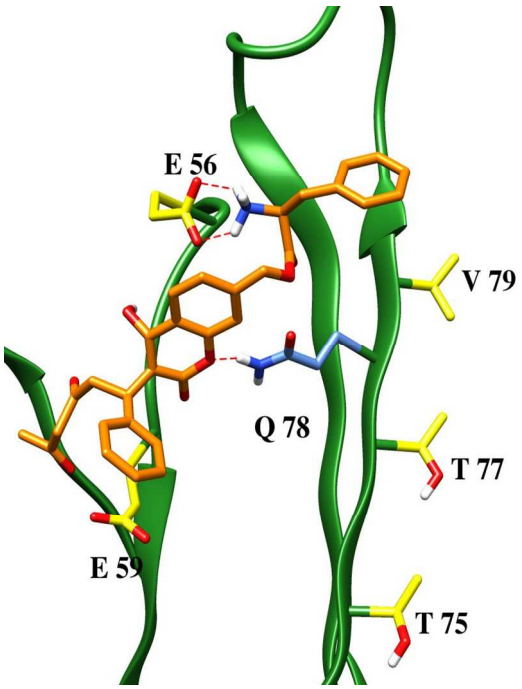

Figure S4. Compound 4 (orange) inside the binding pocket of Axl receptor. The receptor is shown in green as a cartoon representation. The key residues are highlighted in yellow. The residues that are different from the key residues, but are involved in contacts with the compound are shown in cornflower blue. The contacts are indicated in red dashed lines.

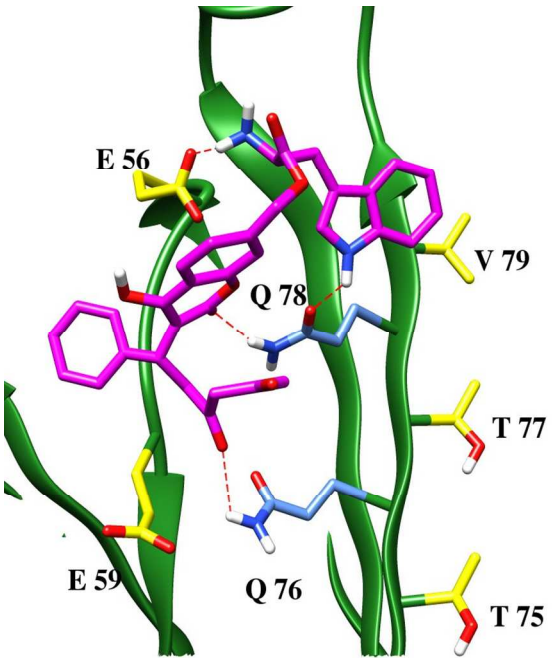

Figure S5. Compound 5 (magenta) inside the binding pocket of Axl receptor. The receptor is shown in green as a cartoon representation. The key residues are highlighted in yellow. The residues that are different from the key residues, but are involved in contacts with the compound are shown in cornflower blue. The contacts are indicated in red dashed lines.

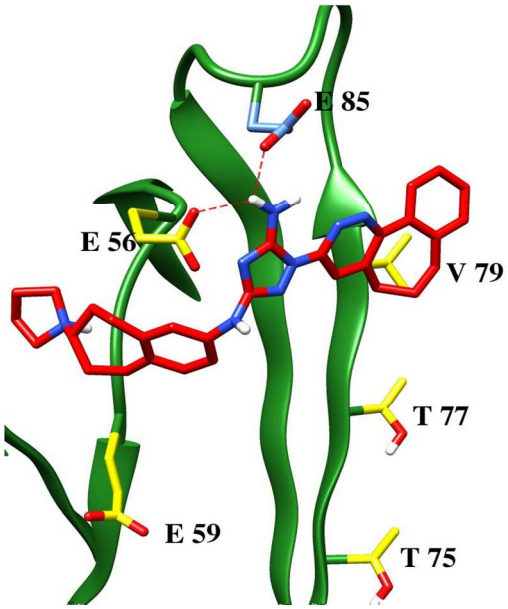

Figure S6. R428 (red) inside the binding pocket of Axl receptor. The receptor is shown in green as a cartoon representation. The key residues are highlighted in yellow. The residues that are different from the key residues, but are involved in contacts with the compound are shown in cornflower blue. The contacts are indicated in red dashed lines.

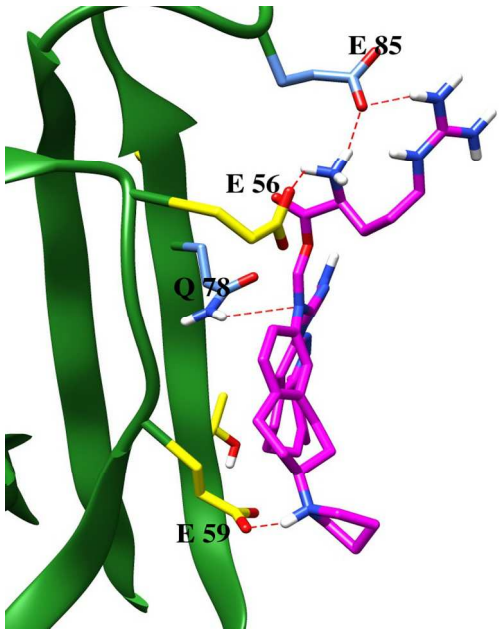

Figure S7. Compound 1' (magenta) inside the binding pocket of Axl receptor. The receptor is shown in green as a cartoon representation. The key residues are highlighted in yellow. The residues that are different from the key residues, but are involved in contacts with the compound are shown in cornflower blue. The contacts are indicated in red dashed lines.

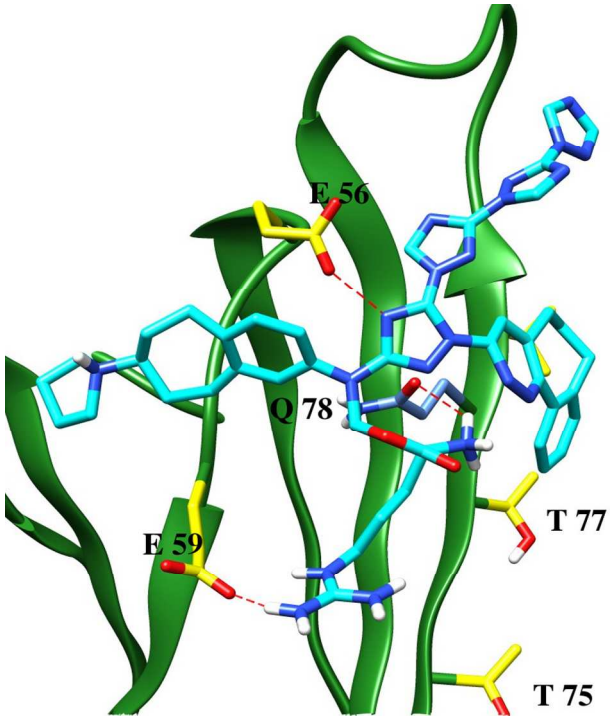

Figure S8. Compound 2' (cyan) inside the binding pocket of Axl receptor. The receptor is shown in green as a cartoon representation. The key residues are highlighted in yellow. The residues that are different from the key residues, but are involved in contacts with the compound are shown in cornflower blue. The contacts are indicated in red dashed lines.

As an important parameter of structural stability, the RMSD value of Axl stabilized after 15 ns. On the contrary, the RMSD value for warfarin remained low except for compound 2', which showed a gradual increase and reached the RMSD level for protein after 30 ns. Additionally, the root mean square fluctuations (RMSF) of warfarin, compound 2' and Axl as a function of the atomic number were plotted to emphasize the average atomic fluctuations during the 50 ns MD simulation time. Similarly, the RMSF value for warfarin showed less atomic fluctuations in comparison to compound 2' due to the small atomic number and higher stability confirmed by RMSD (S9C). The RMSF parameter of Axl represented almost identical atomic movements either in complex with warfarin or compound 2' (S9D) followed by the absence of significant secondary structure changes (S10 A, B).

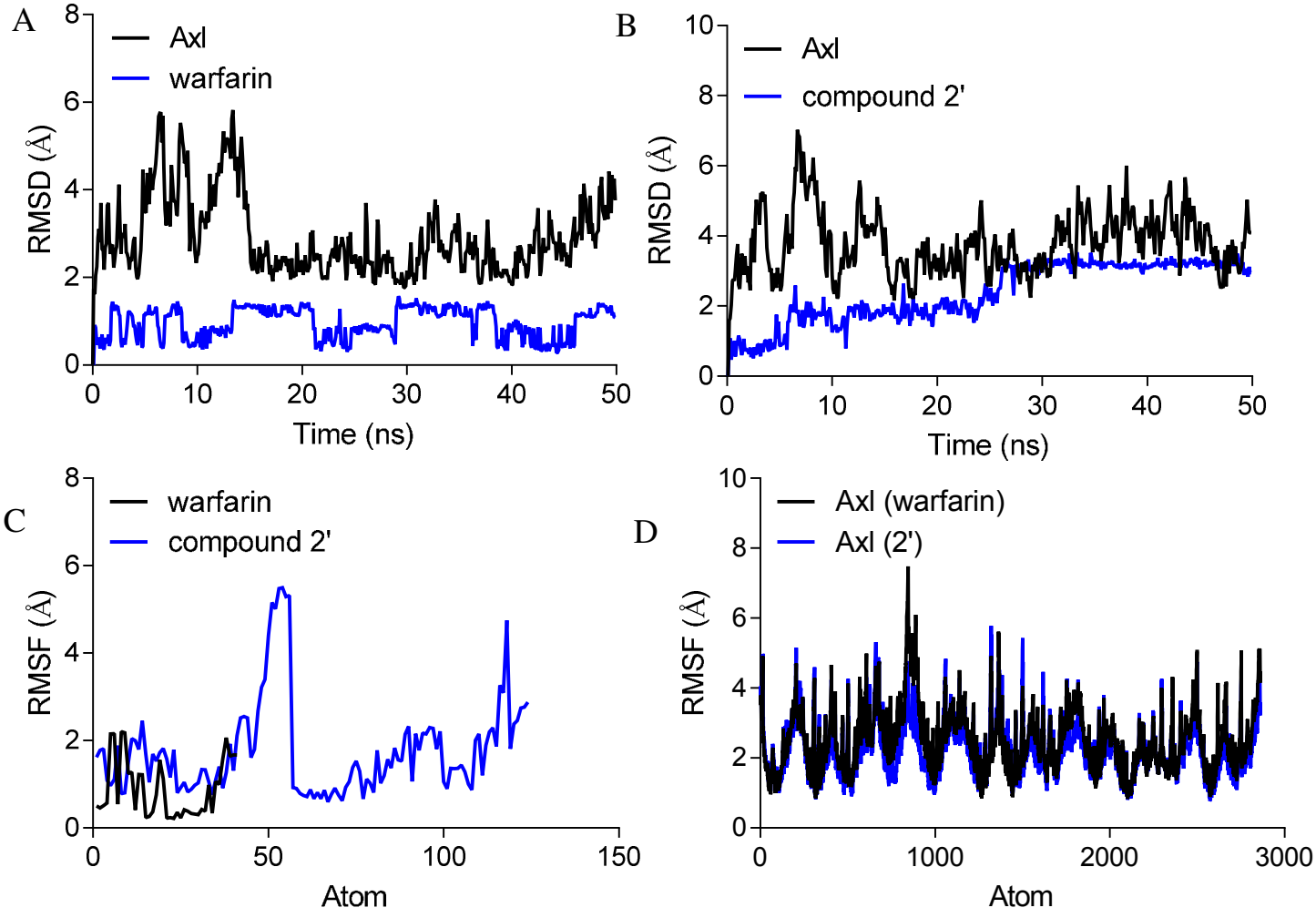

Figure S9. RMSD (A, B) and RMSF (C, D) values for warfarin, compound 2', and Axl receptor during a 50 ns (nanoseconds) MD simulation.

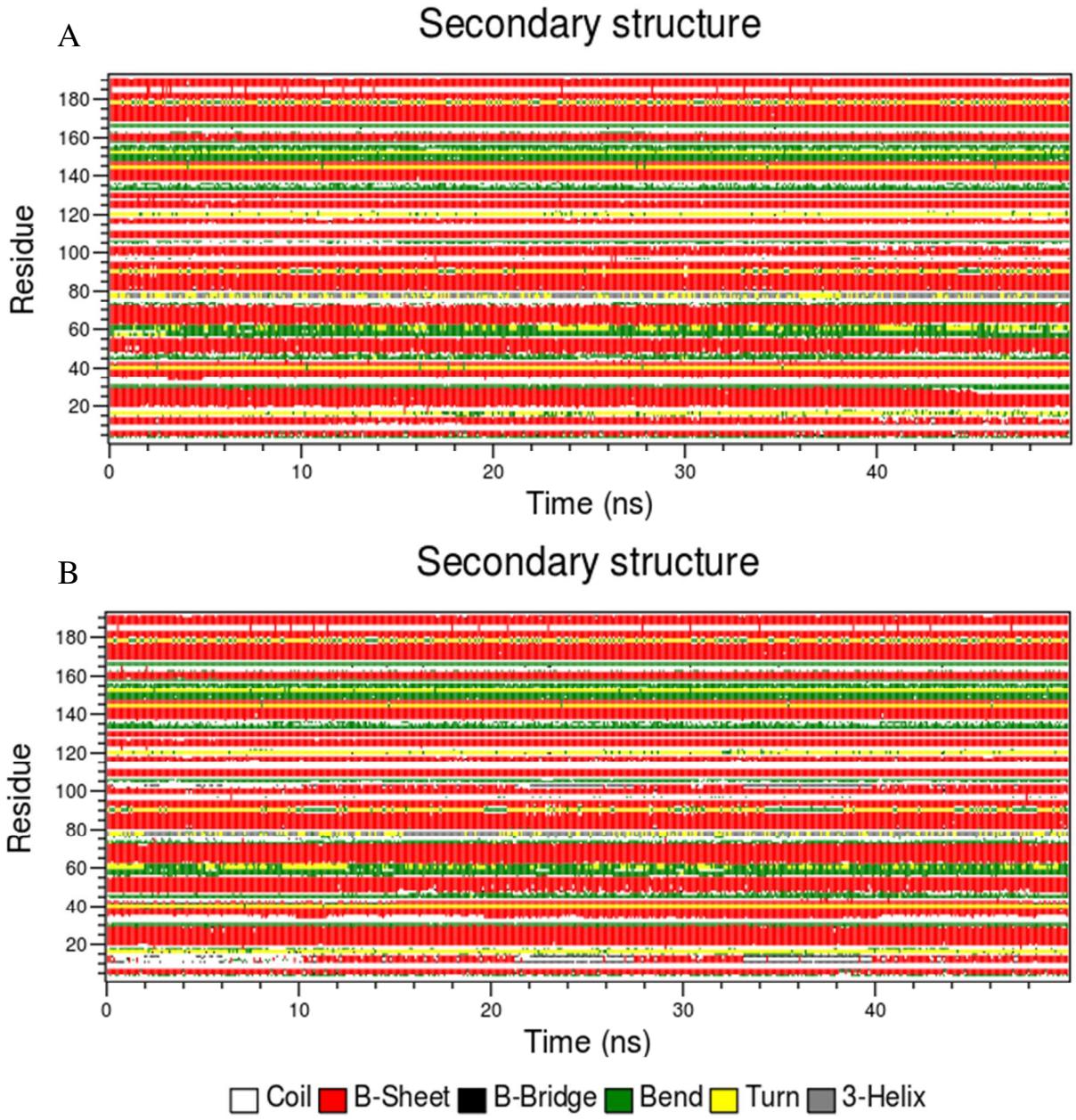

Figure S10. Secondary structure analysis using the hydrogen bond estimation algorithm (DSSP) of Axl receptor bound to the warfarin (A) or compound 2' (B) molecules to investigate the protein structural fluctuations as a function of time.

Table S1. The closest distances between the compounds and residues inside the binding cavity that are involved in interactions.

Compound	***Residue***	***Distance, Å***
1	Q78	1.79
2	Q78	2.62
3	E56 Q78	1.76 1.92
4	E56 (1) E56 (2) Q78	1.77 1.81 1.83
5	E56 Q78 (1) Q78 (2) Q76	2.07 1.97 1.88 3.01
R428	E85 E56	2.14 2.84
1'	E85 (1) E82 (2) E56 Q78 E59	2.1 2.23 2.13 2.97 2.07
2'	E56 E59 Q78	2.63 1.98 2.48